

Supplementary Information

Nanosheets of MIL-53(Al) applied in membranes with improved CO₂/N₂ and CO₂/CH₄ selectivities

Adelaida Perea-Cachero,^a Javier Sánchez-Laínez,^a Beatriz Zornoza,^a Enrique Romero-Pascual,^b Carlos Téllez^a and Joaquín Coronas^{a,*}

^a Chemical and Environmental Engineering Department and Instituto de Nanociencia de Aragón (INA), Universidad de Zaragoza, 50018 Zaragoza, Spain

^b Chemical and Environmental Engineering Department and Aragón Institute of Engineering Research (I3A), Universidad de Zaragoza, 50018 Zaragoza, Spain

*Corresponding author: coronas@unizar.es

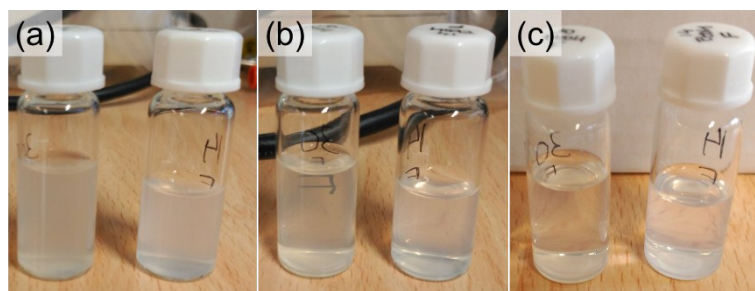


Fig. S1. Photographs of suspensions of ST-RT-30d-ns (left) and REF-60°C-14d-ns (right) in ethanol (ca. 1 mg mL⁻¹) after (a) 0, (b) 1 and (c) 21 d.

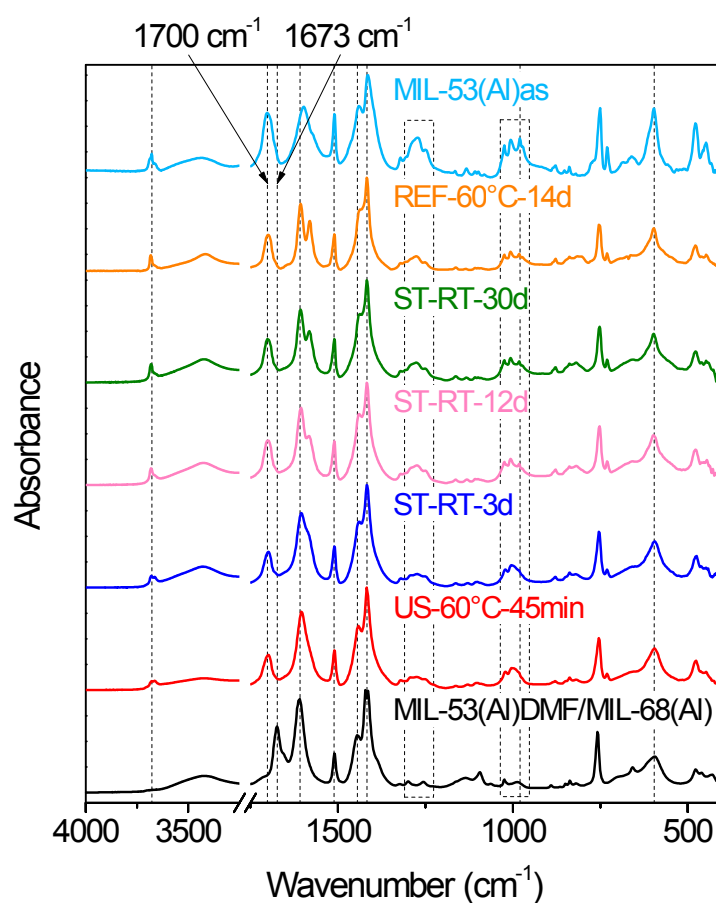


Fig. S2. FTIR spectra of MIL-53(Al)DMF/MIL-68(Al), MIL-53(Al)as and the intermediate products using different immersion conditions. The band at 1700 cm⁻¹ in MIL-53(Al)as corresponds to the carbonyl (C=O) group from the free terephthalic acid trapped in the pores during the synthesis. In MIL-53(Al)DMF/MIL-68(Al) this band could be hidden by a more intense signal placed at 1673 cm⁻¹ related to the carbonyl group from the DMF present in the cavities. The bands at 1609 and 1511 cm⁻¹ in MIL-53(Al)DMF/MIL-68(Al) (1598 and 1510 cm⁻¹ in MIL-53(Al)as) were related to the asymmetric stretching of carboxylates coordinated to aluminium (COO-Al) while bands placed at 1445 and 1417 cm⁻¹ (1440 and 1415 cm⁻¹ in MIL-53(Al)as) were ascribed to the symmetric stretching.¹ The peak at 988 cm⁻¹, weak in MIL-53(Al)DMF/MIL-68(Al) and strong in MIL-53(Al)as (980 cm⁻¹), was assigned to the bending vibration of AlO₄(OH)₂ μ₂-hydroxo groups.² ³ A weak band at 3682 cm⁻¹ appeared in MIL-53(Al)as attributed to the stretching vibration of these groups.³ The bands sited within the wavenumber ranges of 1336-1218 cm⁻¹ and 1054-937

cm^{-1} were more intense for MIL-53(Al)as. In addition, the signal placed at 598 cm^{-1} was stronger and sharper for MIL-53(Al)as than for the mixture MIL-53(Al)DMF/MIL-68(Al) (595 cm^{-1}).

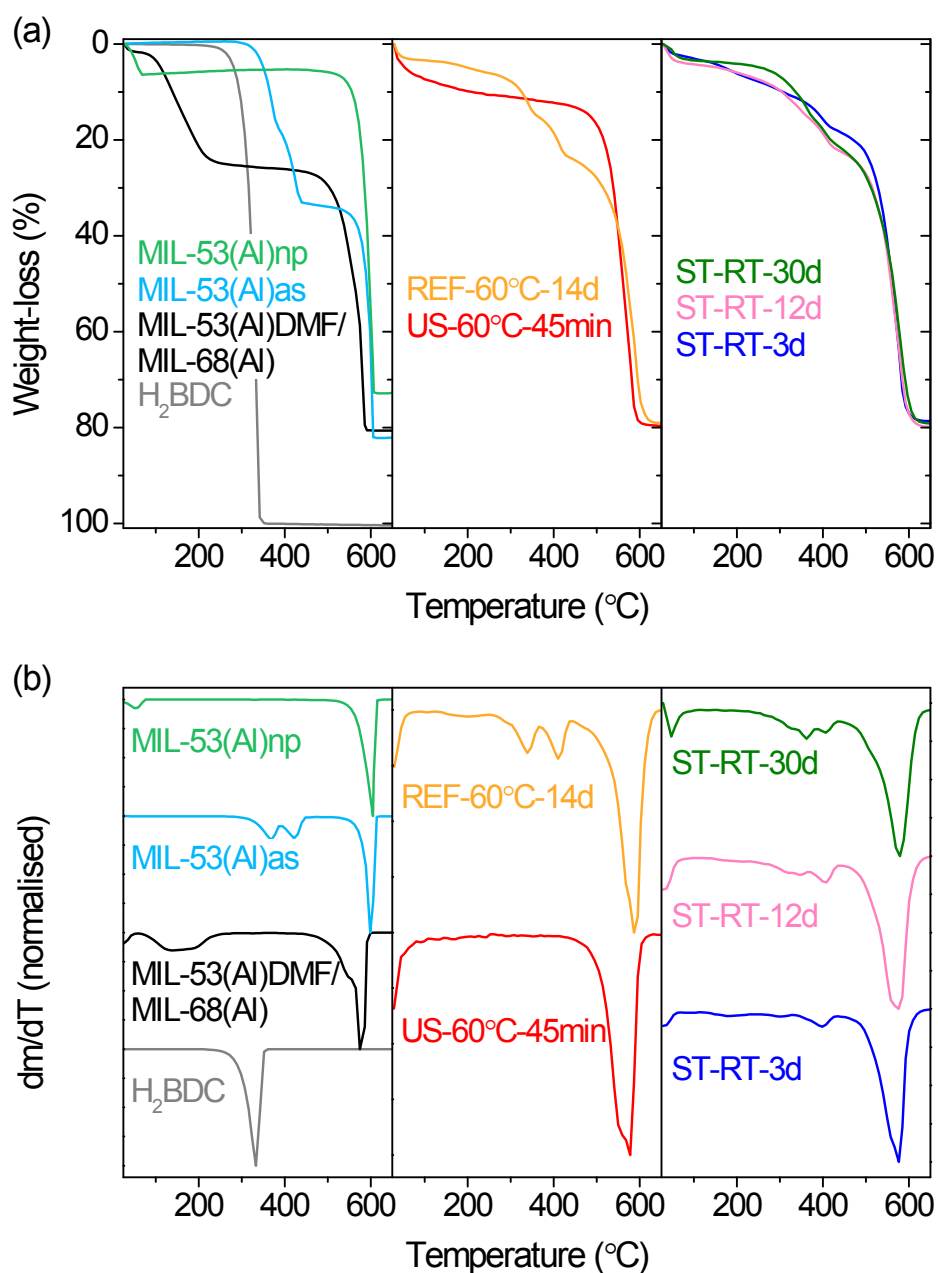


Fig. S3. (a) TGA and (b) DTG curves of H₂BDC, MIL-53(Al)DMF/MIL-68(Al), MIL-53(Al)as, MIL-53(Al)np and the intermediate products.

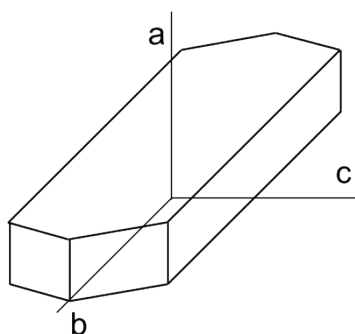


Fig. S4. Schematic representation of the typical morphology of MIL-53(Al) crystals.

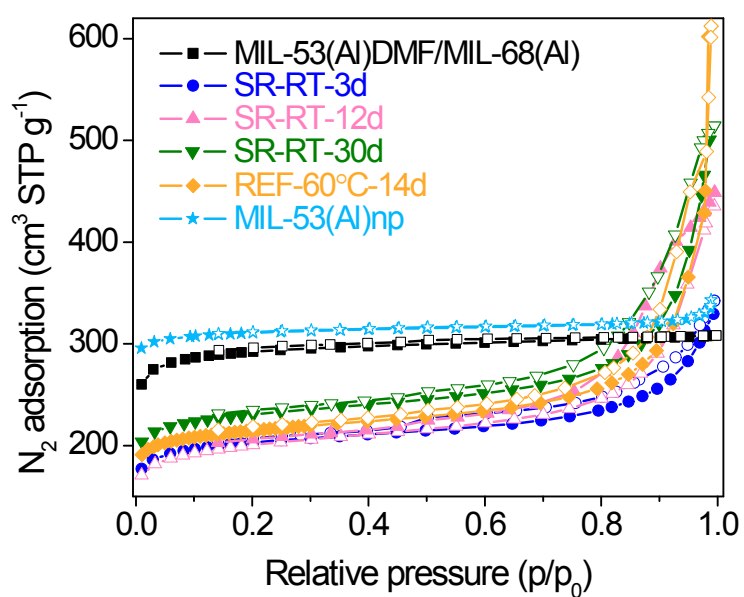


Fig. S5. N₂ sorption isotherms of MIL-53(Al)np, MIL-53(Al)DMF/MIL-68(Al) and the intermediate products.

Table S1. External (S_{ext}) and BET surface (S_{BET}) areas of the intermediate products, MIL-53(Al)DMF/MIL-68(Al) and MIL-53(Al)np.

MOF	S_{BET} (m ² g ⁻¹)	S_{ext} (m ² g ⁻¹)	Reference
MIL-53(Al)DMF/MIL-68(Al)	1121	122	This work
ST-RT-3d	772	134	This work
ST-RT-12d	757	153	This work
ST-RT-30d	875	151	This work
REF-60°C-14d	828	141	This work
MIL-53(Al)np	1051	69	This work
MIL-68(Al)	1430	-	4
MIL-53(Al)np	1140	-	5

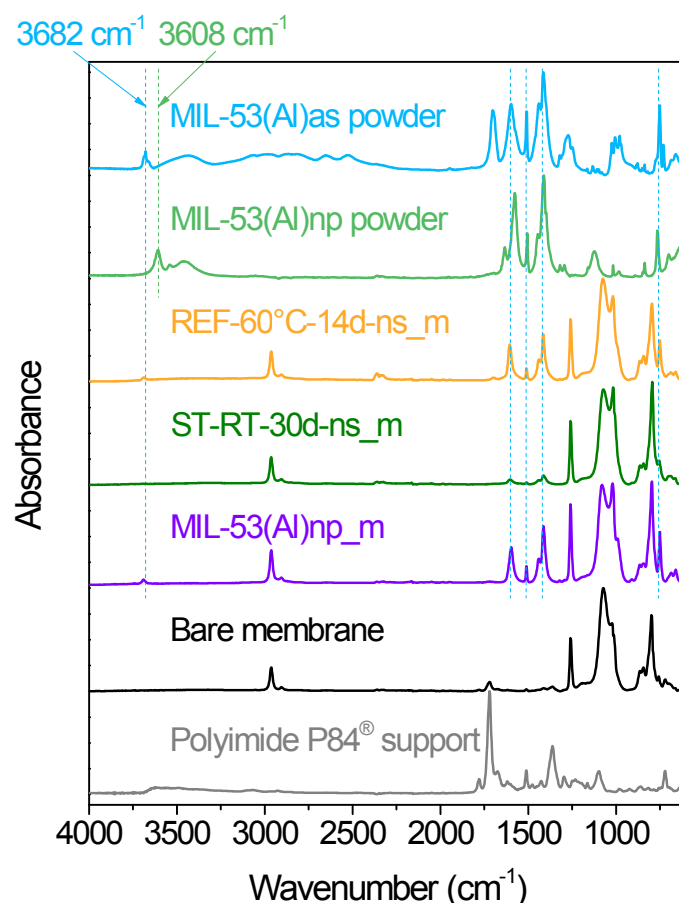


Fig. S6. FTIR spectra of MIL-53(Al)as and MIL-53(Al)np powders. ATR-FTIR spectra of the bare membrane, MIL-53(Al)np_m, ST-RT-30d-ns_m and REF-60°C-14d-ns_m. The ATR-FTIR spectrum of the P84[®] support presented the characteristic bands of polyimides. The bands placed at 1781 and 1720 cm^{-1} were due to the asymmetric and symmetric stretching of carbonyl function in the imide group.⁶ The signal at 1363 cm^{-1} corresponded to the stretching of C-N, while the band at 862 cm^{-1} was assigned to the deformation of the imide group.⁶ The bands at 1097 and 722 cm^{-1} were consequence of the transverse and out-of-plane vibration of the cyclic imide.⁷ The bare membrane was fabricated covering the polyimide support by PDMS upon vacuum filtration. The main signals appearing in the corresponding spectrum were attributed to PDMS. The band at 2962 cm^{-1} was assigned to the stretching of trimethylsilyl (Si-CH₃) functions.⁸ The bands at 1072 and 864 cm^{-1} were due to the stretching of siloxane (Si-O-Si) and silanol (Si-OH) groups, respectively.⁸ Only the weak signal at 1720 cm^{-1} was assigned to the polyimide support (symmetric stretching of carbonyl groups). The spectra of the membranes prepared with MIL-53(Al)np and REF-60°C-14d-ns (MIL-53(Al)np_m and REF-60°C-14d-ns_m) revealed the presence of these MOF materials since the bands at 1598 and 1510 cm^{-1} (asymmetric stretching of carboxylates coordinated to aluminium) and 1415 cm^{-1} (symmetric stretching) were seen. ST-RT-30d-ns_m also presented those bands but their intensity was much lower. The contribution of PDMS in the three membranes was observed with the appearance of all its characteristic signals. The band for the stretching vibration of $\text{AlO}_4(\text{OH})_2 \mu_2$ -hydroxo groups appeared at 3608 cm^{-1} in the MIL-53(Al)np powder while the same signal was at 3682 cm^{-1} in MIL-53(Al)as. Thus, a shift towards lower wavenumbers was provoked when activating MIL-53(Al)as to MIL-53(Al)np. Since the membranes were fabricated using activated intermediate and MIL-53(Al)np

products, the corresponding spectra should have shown a band around 3608 cm^{-1} , as in the MIL-53(Al)np spectrum. Nonetheless, the signal arose at 3682 cm^{-1} , as in the case of MIL-53(Al)as. This could be related to the typical breathing effect of MIL-53(Al). As mentioned above, during activation terephthalic acid molecules are released from the pores of MIL-53(Al)as and, thus, the intermediate products, leading to empty large pores. After exposure to atmosphere, the pores adsorb water molecules producing a contraction owing to interactions between the pore walls and water molecules. Therefore, polymeric chains of PDMS could have penetrated into the outer pores of the MOF crystals during membrane preparation, causing pore expansion and giving a structure as open as that of MIL-53(Al)as.

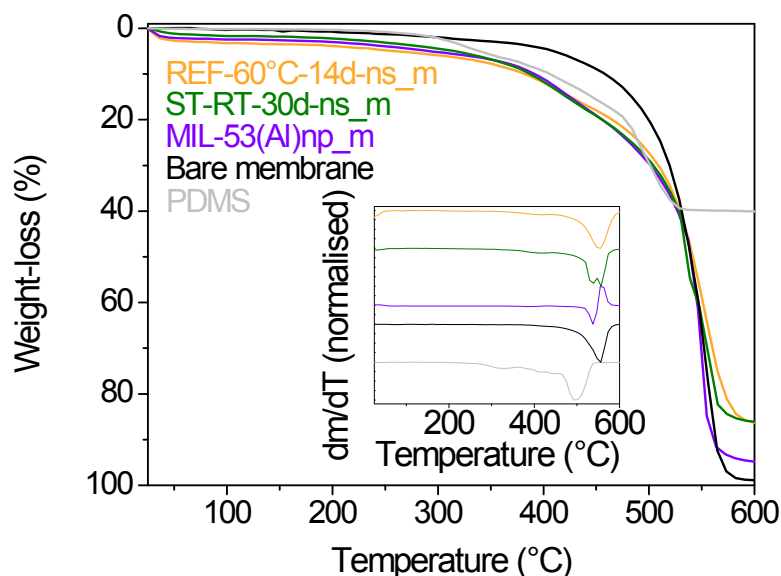


Fig. S7. TGA and DTG curves of the membranes prepared in this work and those of PDMS. The thermogram of the bare membrane presented a plateau up to $340\text{ }^{\circ}\text{C}$ (2.8 %) and a step of 4.5 % between 340 and $440\text{ }^{\circ}\text{C}$. These mass losses were assigned to n-hexane and PDMS, respectively. The bare membrane degraded above $440\text{ }^{\circ}\text{C}$. The thermograms of the membranes with the intermediate materials were similar. They had a small weight loss below $100\text{ }^{\circ}\text{C}$ (1.8 and 3.0 % for ST-RT-30d-ns_m and REF-60°C-14d-ns_m, respectively) attributed to water adsorbed from atmosphere. The second step from 100 to $250\text{ }^{\circ}\text{C}$ (2.5 and 3.0 %, respectively) corresponded to the n-hexane molecules from membrane preparation. These membranes also had a weight loss between 250 and $440\text{ }^{\circ}\text{C}$ (14.1 and 10.6 %, respectively) related to PDMS, as in the case of the bare membrane. The thermogram of MIL-53(Al)np_m showed weight losses of 2.6, 2.5 and 11.6 % between 25 - $100\text{ }^{\circ}\text{C}$, 140 - $300\text{ }^{\circ}\text{C}$ and 300 - $440\text{ }^{\circ}\text{C}$ assigned to water, n-hexane and PDMS, respectively. The zig-zag shape at 500 - $600\text{ }^{\circ}\text{C}$ in the DTG curve of MIL-53(Al)np_m was caused by sharply degradation. The weight losses corresponding to PDMS in the three MMMs were higher than that of the bare membrane (4.5 %). The cure reaction of PDMS starts with the mixing process of the base and the curing agent and finishes with the heat treatment. The incorporation of particles interfered with the cross-linking of PDMS at the heat curing stage and made PDMS less cross-linked.^{9, 10} Thus, the PDMS of the MMMs was easier to decompose into smaller and more volatile products, resulting in a faster weight loss.^{9, 10} The higher percentage of inorganic residue (Al_2O_3 and SiO_2) of ST-RT-30d-ns_m and REF-60°C-14d-

ns_m (53.7 and 50.1 %, respectively) compared to that of MIL-53(Al)np_m (17.2 %) implied a higher content of MOF and/or PDMS.

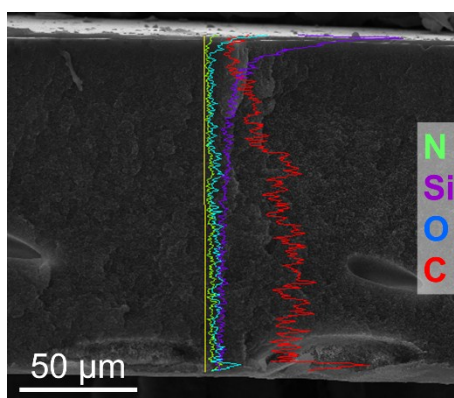


Fig. S8. Composition line SEM image of the bare membrane.

Table S2. Comparison between permeance and selectivity values of a dense PDMS membrane tested under single gas conditions and for CO₂/CH₄ and CO₂/N₂ separation mixtures.

Analysis	Permeance (GPU)			Selectivity	
	CO ₂	N ₂	CH ₄	CO ₂ /N ₂	CO ₂ /CH ₄
Single gas	18.1	4.6	3.4	11.1	5.3
Mixed gas (CO ₂ /N ₂)	15.9	1.6	-	10.0	-
Mixed gas (CO ₂ /CH ₄)	19.9	-	3.9	-	5.1

Table S3. Permeance and selectivity values of the different membranes for CO₂/CH₄ and CO₂/N₂ separation mixtures.

Membrane	Permeance (GPU)		Selectivity	Permeance (GPU)		Selectivity
	CO ₂	CH ₄	CO ₂ /CH ₄	CO ₂	N ₂	CO ₂ /N ₂
Bare membrane	47.5	4.4	10.8	61.9	7.0	8.9
MIL-53(Al)np_m	9.5	0.4	22.4	11.2	0.6	17.5
ST-RT-30d-ns_m	20.8	0.7	28.4	17.7	0.9	19.9
REF-60°C-14d-ns_m	29.6	1.0	28.7	26.8	1.2	23.2

Table S4. Variations (%) of permeance and selectivity in comparison to the bare membrane.

Membrane	Permeance (GPU)		Selectivity	Permeance (GPU)		Selectivity
	CO ₂	CH ₄	CO ₂ /CH ₄	CO ₂	N ₂	CO ₂ /N ₂
MIL-53(Al)np_m	-80	-90	107	-82	-91	97
ST-RT-30d-ns_m	-56	-83	162	-71	-87	125
REF-60°C-14d-ns_m	-38	-77	165	-57	-83	161

Table S5. Comparison of permeability and selectivity values for selected MMMs prepared with MIL-53(Al) materials or PDMS in CO₂/CH₄ separation.

MOF	Polymer	Δp (bar)	T (°C)	Gas permeation experiment			Reference
				Single		Binary	
				P CO ₂ (Barrer)	α CO ₂ /j	α CO ₂ /j	
MIL-53(Al)	PI Matrimid®	10.3	35	6.2-6.7	9.4-31.0	8.5-28.5	11
		6	25	0.3 GPU	72.1	-	12
		6	25	0.2 GPU	50.5	-	
	PEI Ultem®	10.3	35	1.5-1.8	39.5-43.1	31.6-42.8	11
	6FDA/ODA-DAM (1/1)	10.3	35	54.1-61.5	12.5-23.5	13.0-23.6	11
	6FDA/ODA-DAM (1/1) + 2% APTMDS	10.3	35	32.2-76.4	8.9-18.9	8.8-20.2	11
	6FDA/ODA-DAM (1/4)	10.3	35	123-130	18.1-23.2	19.1-23.6	11
	M-PVDF	5	25	1.2-2.5	27.9-39.6	-	13
NH ₂ -MIL-53(Al)	PI Matrimid®	10.3	35	9.2	2.1	2.1	11
	PEI Ultem®	10.3	35	3.0	36.2	36.1	11
	6FDA/ODA-DAM (1/1)	10.3	35	50.0-52.6	12.5-34.1	12.5-31.8	11
	6FDA/ODA-DAM (1/1) + 2% APTMDS	10.3	35	49.9-65.8	20.8-36.6	20.0-33.9	11
	6FDA/ODA-DAM (1/4)	10.3	35	112-115	14.1-28.2	14.3-28.5	11
	M-PVDF	5	25	1.7-2.2	37.6-43.9	-	13
HKUST-1	PDMS	-	-	-	8.9	-	14
ST-RT-30d-ns_m	PDMS	2	35	20.8 GPU ^a 141.3 ^b	-	28.4	This work
REF-60°C-14d-ns_m	PDMS	2	35	29.6 GPU ^a 159.6 ^b	-	28.7	This work

P, permeability (Barrer) or permeance (GPU); α , selectivity (ideal selectivity when single gas permeation tests); PI, polyimide; PEI, polyetherimide; 6FDA, 4,4'-(hexafluoroisopropylidene)-diphthalic anhydride; ODA, 4,4'-oxidianiline; DAM, 1,3,5-trimethyl-2,6-phenylenediamine; APTMDS, bis(3-aminopropyl)tetramethyldisiloxane; M-PVDF, modified poly(vinylidene fluoride).

^a CO₂ permeance value in the CO₂/CH₄ binary gas permeation experiment.

^b CO₂ permeability value (Barrer) in the CO₂/CH₄ binary gas permeation experiment calculated using the corresponding MMM thickness obtained from cross-sectional SEM images.

Table S6. Comparison of permeability and selectivity values for MMMs prepared with MIL-53(Al) materials or PDMS in CO₂/N₂ separation.

MOF	Polymer	Δp (bar)	T (°C)	Gas permeation experiment			Reference
				Single		Binary	
				P CO ₂ (GPU)	α CO ₂ /j	α CO ₂ /j	
MIL-53(Al)	PI Matrimid®	6	25	0.3	34.8	-	12
		6	25	0.2	27.5	-	
	PEI Ultem®	5	25	9.1-27.7	31.0-41.8	-	15
HKUST-1	PDMS	-	-	-	3.4	-	14
ST-RT-30d-ns_m	PDMS	2	35	17.7 ^a	-	19.9	This work
REF-60°C-14d-ns_m	PDMS	2	35	26.8 ^a	-	23.2	This work

P, permeance (GPU); α , selectivity (ideal selectivity when single gas permeation experiments); PI, polyimide; PEI, polyetherimide.

^a CO₂ permeance value in the CO₂/N₂ binary gas permeation experiment.

References

1. P. Rallapalli, D. Patil, K. P. Prasanth, R. S. Somani, R. V. Jasra, H. C. Bajaj, *J. Porous Mater.*, 2010, **17**, 523-528.
2. C. Volkringer, T. Loiseau, N. Guillou, G. Ferey, E. Elkaim, A. Vimont, *Dalton Trans.*, 2009, 2241-2249.
3. J. Liu, F. Zhang, X. Zou, G. Yu, N. Zhao, S. Fan, G. Zhu, *Chem. Commun.*, 2013, **49**, 7430-7432.
4. Q. Yang, S. Vaesen, M. Vishnuvarthan, F. Ragon, C. Serre, A. Vimont, M. Daturi, G. De Weireld, G. Maurin, *J. Mater. Chem.*, 2012, **22**, 10210-10220.
5. T. Loiseau, C. Serre, C. Huguenard, G. Fink, F. Taulelle, M. Henry, T. Bataille, G. Ferey, *Chem. - Eur. J.*, 2004, **10**, 1373-1382.
6. S. H. Choi, J. C. Jansen, F. Tasselli, G. Barbieri, E. Drioli, *Sep. Purif. Technol.*, 2010, **76**, 132-139.
7. Y. Liu, T. S. Chung, R. Wang, D. F. Li, M. L. Chng, *Ind. Eng. Chem. Res.*, 2003, **42**, 1190-1195.
8. W. S. Hanoosh, E. M. Abdelrazaq, *Malay. Polym. J.*, 2009, **4**, 52-61.
9. S. Y. Lu, C. P. Chiu, H. Y. Huang, *J. Membr. Sci.*, 2000, **176**, 159-167.
10. S. Y. Lu, H. Y. Huang, K. H. Wu, *J. Mater. Res.*, 2001, **16**, 3053-3059.